Behavioral/Cognitive

Cortical Thinning Explains Changes in Sleep Slow Waves during Adulthood

Jonathan Dubé,[1,2,3] Marjolaine Lafortune,[2] Christophe Bedetti,[2,3] Maude Bouchard,[1,2,3] Jean François Gagnon,[2,4] Julien Doyon,[1,3] Alan C. Evans,[5] Jean-Marc Lina,[6,7] and Julie Carrier[1,2,3]

[1]Department of Psychology, Université de Montréal, Montréal H2V 2S9, Canada, [2]Center for Advanced Research in Sleep Medicine, Hôpital du Sacré-Cœur de Montréal, Montréal H4J 1C5, Canada, [3]Centre de Recherche de l'Institut Universitaire de Gériatrie de Montréal, Montréal H3W 1W4, Canada, [4]Department of Psychology, Université du Québec à Montréal, Montréal H2L 2C4, Canada, [5]Montreal Neurological Institute, McGill University, Montréal H3A 2B4, Canada, [6]Department of Electrical Engineering, École de Technologie Supérieure, Montréal H3C 1K3, Canada, and [7]Centre de Recherches Mathématiques, Université de Montréal, Montréal H3C 1K3, Canada

Sleep slow waves (SWs) change considerably throughout normal aging. In humans, SWs are generated and propagate on a structural backbone of highly interconnected cortical regions that form most of the default mode network, such as the insula, cingulate cortices, temporal lobe, parietal lobe, and medial frontal lobe. Regions in this network undergo cortical thinning and breakdown in structural and functional connectivity over the course of normal aging. In this study, we investigated how changes in cortical thickness (CT), a measure of gray matter integrity, are involved in modifications of sleep SWs during adulthood in humans. Thirty young (mean age = 23.49 years; SD = 2.79) and 33 older (mean age = 60.35 years; SD = 5.71) healthy subjects underwent a nocturnal polysomnography and T1 MRI. We show that, when controlling for age, higher SW density (nb/min of nonrapid eye movement sleep) was associated with higher CT in cortical regions involved in SW generation surrounding the lateral fissure (insula, superior temporal, parietal, middle frontal), whereas higher SW amplitude was associated with higher CT in middle frontal, medial prefrontal, and medial posterior regions. Mediation analyses demonstrated that thinning in a network of cortical regions involved in SW generation and propagation, but also in cognitive functions, explained the age-related decrease in SW density and amplitude. Altogether, our results suggest that microstructural degradation of specific cortical regions compromise SW generation and propagation in older subjects, critically contributing to age-related changes in SW oscillations.

Key words: **aging; cortical thickness; electroencephalography; humans; sleep; slow waves**

Introduction

Sleep slow waves (SWs; <4 Hz, >75 μV) on the electroencephalogram (EEG) are a hallmark feature of nonrapid eye movement (NREM) sleep. These waves reflect a synchronized slow oscillation in cortical neurons between a depolarization (active) state and a hyperpolarization (silent) state (Steriade et al., 1993b). As neurons go through intense synaptic activity during waking, opportunity for neural silence in the silent state is hypothesized to allow for the cell's rest, promoting prophylactic maintenance at the cellular level and functional restoration at the network level (Vyazovskiy and Harris, 2013). It is suggested that such a homeostatic response remodels neural networks and restores the brain's capacity for plasticity (Tononi and Cirelli, 2014).

Animal studies have shown that the cellular states underlying SWs are generated locally before spreading to cortical networks (Chauvette et al., 2010). Whereas the silent state takes place nearly instantaneously in most neurons, the active state tends to first occur in specific neurons and then propagate (Volgushev et al., 2006). A similar pattern takes place on EEG recordings. Each EEG SW originates from a definite location, usually in anterior regions, and then sweeps across the cortex as a traveling wave (Massimini et al., 2004). Depth electrode recordings in humans also showed that SW active states start preferentially in frontal regions before spreading posteriorly (Nir et al., 2011). EEG source analysis showed that neural activity underlying SWs begins most frequently in the insula, in the anterior cingulate, or around the lateral fissure (Murphy et al., 2009). Subsequently, SWs grow in amplitude while their neural activity spreads in the default-mode network (DMN) between its anterior (anterior cingulate, medial/middle frontal) and posterior (posterior cingulate, precuneus) nodes. SWs also involve hemodynamic responses in the DMN (Dang Vu et al., 2008).

During adulthood, decreases in SW density, amplitude, and slope occur predominantly in frontal regions, suggesting impair-

Received Sept. 20, 2014; revised March 25, 2015; accepted April 3, 2015.

Author contributions: J. Dubé, M.L., and M.B. performed research; J. Dubé, C.B., J.F.G., J. Doyon, A.C.E., and J.-M.L. contributed unpublished reagents/analytic tools; J. Dubé analyzed data; J. Dubé wrote the paper; J.C. designed research.

This work was supported by the Canadian Institutes of Health Research (CIHR) Grant 93733 to J.C. and CIHR scholarships and Fonds de Recherche du Québec en Santé to J. Dubé, M.L., M.B., J.F.G., and J.C.. We thank Florin Amzica for thoughtful comments on the manuscript.

The authors declare no competing financial interests.

Correspondence should be addressed to Julie Carrier, PhD, Center for Advanced Research in Sleep Medicine, Hôpital du Sacré-Cœur de Montréal, 5400 Gouin West Blvd., Montreal, Québec H4J 1C5, Canada. E-mail: julie.carrier.1@umontreal.ca.

DOI:10.1523/JNEUROSCI.3956-14.2015

 0270-6474/15/357795-14$15.00/0

ment in cortical circuits underlying SWs (Carrier et al., 2011). Neuroimaging studies showed consistent age-related cortical thinning in frontal regions and in the DMN (Fjell et al., 2009). Nonpathological cortical thinning is thought to reflect cell body shrinkage and reduction in the dendritic arborization and synaptic density of cortical neurons (Salat et al., 2004). Because synchronized neural activity during SWs is generated cortically (Steriade et al., 1993a), gray matter atrophy could trigger age-related changes in SWs.

Accordingly, human studies showed that the decrease of slow-wave activity (SWA) in adolescence occurs in parallel with cortical thinning in frontal, parietal, and temporal areas (Buchmann et al., 2011b). Moreover, higher SW density and amplitude in adults is associated with greater gray matter (as shown by voxel-based morphometry) in similar cortical areas and in the hypothalamus (Saletin et al., 2013). Interestingly, region-of-interest studies showed that atrophy of the medial prefrontal cortex was linked to SWA decline in the elderly (Mander et al., 2013). However, because SWs arise from synchronized activity in cortical networks, we hypothesized that changes in other cortical regions where SW source activity begins and propagates would explain the decrease of SW density, amplitude, and slope during adulthood.

Materials and Methods

Participants

Sixty-three healthy participants divided into two age groups, 30 young (16 men/14 women; 20–30 years old; mean age = 23.49 years; SD = 2.79) and 33 older (15 men/18 women; 50–70 years old, mean age = 60.35 years; SD = 5.71) adults, participated in this study. A homemade questionnaire and a semistructured interview were used to exclude potential subjects who smoked, used medication known to affect the sleep–wake cycle or the CNS, complained about their sleep–wake cycle or cognition, and/or reported habitual sleep duration of <7 h or >9 h. Subjects were also excluded if they had any history of neurological or psychiatric disorders. Potential subjects with a score of >13 on the Beck Depression Inventory were also excluded (Beck et al., 1988). Moreover, participants underwent a neuropsychological assessment to exclude any cognitive impairment or dementia diagnosis (American Psychiatric Association, 2000). Before the polysomnographic (PSG) night used for analyses, participants underwent an adaptation and screening full-night PSG, including recordings from a nasal/oral thermistor and leg electromyogram to screen for sleep disturbances. The presence of sleep apneas and hypopneas (index per hour >10) and periodic leg movements (index per hour >10) resulted in the exclusion of the participant. Premenopausal women using hormonal contraceptives or receiving hormonal replacement therapy were also excluded. We ensured that premenopausal women reported regular menstrual cycles (25–32 d) during the year preceding the study and had no vasomotor complaints (i.e., hot flashes, night sweats). All procedures were approved by the ethics committee of Hôpital du Sacré-Coeur de Montréal and of the Unité de NeuroImagerie Fonctionelle in Montreal, Canada. Subjects signed an informed consent form and received monetary compensation.

Procedures

Sleep EEG. Subjects underwent nocturnal PSG at habitual bedtimes based on subjective reporting. Subjects had to follow a regular sleep–wake cycle based on their habitual wake times and bedtimes ($\pm$30 min). Twenty EEG electrodes (international 10–20 system; all referenced to linked earlobes), left and right electrooculogram, and submental electromyogram were recorded using a Grass Model 15A54 amplifier system (EEG: gain 10,000; band-pass 0.3–100 Hz; -6 dB). Signals were digitalized at a sampling rate of 256 Hz using commercial software (Harmonie; Stellate Systems). Sleep stages were visually scored in 30 s epochs on a computer screen (Harmonie; Stellate Systems) according to standard criteria (Iber, et al., 2007). Sleep stage variables were computed from sleep onset to last awakening. Sleep efficiency was defined as follows: (number of minutes spent asleep/total number of minutes from sleep onset to last awakening) $\times$ 100. Artifacts were detected automatically and rejected from analysis (Brunner et al., 1996). Further artifacts were eliminated by visual inspection.

Detection of sleep SWs. SWs were detected automatically on artifact-free NREM in both left and right parasagittal scalp derivations (Fp1, Fp2, F3, F4, C3, C4, P3, P4, O1, and O2). Data were initially filtered between 0.3 and 4.0 Hz using a band-pass filter (-3 dB at 0.3 and 4.0 Hz; -23 dB at 0.1 and 4.2 Hz). SWs for each derivation were detected on artifact-free NREM sleep using the following previously published criteria: (1) negative peak <-40 μV, (2) peak-to-peak amplitude >75 μV, (3) duration of negative deflection >125 ms and <1500 ms, and (4) duration of positive deflection <1000 ms (Dang Vu et al., 2008). For each derivation, SW density was defined as the number of SWs per minute of N2 and N3 sleep stages. For each SW, amplitude (defined as the difference in voltage between negative and positive peaks of unfiltered signal expressed in microvolts) and slope between the positive and the negative peaks (in microvolts per second) were derived. Characteristics of SWs were averaged over all-night NREM sleep and between hemispheres (prefrontal: FP1–FP2, frontal: F3–F4, central: C3–C4, parietal: P3–P4, occipital: O1–O2). Because the effects of age on SW characteristics are preeminent into the first NREM period (NREMP) compared with the rest of the night (Carrier et al., 2011), we also computed SW characteristics in frontal derivations for the first NREMP. Sleep cycles were determined according to previously published criteria (Aeschbach and Borbély, 1993). A cycle was defined as an NREM sleep period lasting at least 15 min, followed by an REM period lasting at least 5 min, except for the first REM period.

MRI. All subjects were MRI scanned to get an anatomical T1-weighted sequence on a Siemens Trio 3 tesla scanner at the Unité de Neuroimagerie Fonctionelle (UNF) in Montreal. We used a MP-RAGE sequence with TE of 2.91 ms, 9° flip angle, TR of 2300 ms, 240 mm field-of-view, 1$\times$1 mm pixel spacing, and a matrix size of 256 $\times$ 240.

Cortical thickness analyses. We investigated surface-based cortical thickness (CT), a measure providing information about the number of synapses per column, as well as glial support and dendritic connections (Schüz and Palm, 1989; Paus et al., 2008). This surface-based metric is derived from MRI images using the automated CIVET pipeline, which applies the Constrained Laplacian Anatomic Segmentation using the Proximity (CLASP) algorithm (Kim et al., 2005; Ad-Dab'bagh et al., 2006). This software package was used to: (1) perform stereotaxic registration of the MRI volumes to the International Consortium for Brain Mapping (ICBM) nonlinear sixth generation target (Grabner et al., 2006), using a 12-parameter linear transformation (Collins et al., 1994) and intensity correction for signal intensity nonuniformity (Sled et al., 1998); (2) classify tissue into gray matter, white matter, and CSF (Tohka et al., 2004); and (3) create surfaces using deformable spherical mesh models for white matter, gray matter, and the midsurface, each consisting of 41,962 vertices for both hemispheres (MacDonald et al., 2000). This provides a reliable metric (in millimeters) of surface CT, defined as the Euclidean distance between gray and white matter surface in the individual native space. Data were quality controlled using figures and reports produced by the pipeline and then smoothed by a 20 mm, full-width at half-maximum, surface-based kernel. A value of 20 mm reportedly has good sensitivity without loss of specificity in group analyses (Zhao et al., 2013). To perform group analyses, anatomical brain MRI images were spatially normalized into the MNI standard template.

Analysis pipeline. This study examined whether age-related local variations in CT explained alterations of SW characteristics for each derivation during adulthood. Figure 1 illustrates the mediation model used to address this question. We hypothesized that age affects SW characteristics in a specific derivation (e.g., frontal; path c) by an initial effect on CT in regions (path a) that are associated with SW sleep oscillations, when the effects of age are controlled for (path b). It is mandatory to control for age to isolate regions where SWs explain residual variance in CT because both SWs and CT are linked to age. We used the Preacher and Hayes framework to test for simple mediation (one CT region as the mediator) and parallel mediation models (CT in several regions as mediators in competition) (Hayes, 2013). This analysis decomposes the total effect of age on SW characteristics (path c) into direct (path c′) and indirect

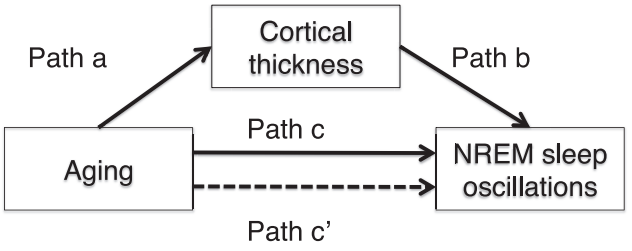

Figure 1. Mediation model. We hypothesized that aging exerts its total effect on SW characteristics (path c) by an initial effect on CT (path a), which then drives changes in NREM sleep oscillations (path b). Mediation occurs when the relationship between aging and sleep oscillations drops significantly when entering the mediators as cofactors in the model (path a*path b = indirect effect). However, it is still possible for age to affect SW characteristics independently of CT through distinct mechanisms (path c′ = direct effect).

effects through specific mediators (indirect effect = ab; therefore, c = c′ + ab). A significant indirect effect indicates mediation–that is, a significant proportion of the age-related effect on SW characteristics is brought about by thinning (or thickening) of a specific region. However, in these models, it is still possible for age to affect SW characteristics independently of CT through distinct mechanisms (path c′ = direct effect). Statistical analyses were performed in five steps (see below) for each SW characteristic (density, amplitude, and slope), in each derivation. Mediation analyses were performed with the PROCESS toolbox version 2.11 under SPSS Statistics for Mac, version 20.

Step 1: Total effect of age on sleep and SW characteristics (path c only)

Preliminary tests of normality revealed that SW variables were not normally distributed in each group ($p < 0.05$, Shapiro–Wilk). Data were successfully log normalized ($p > 0.05$, Shapiro–Wilk). Effects of age on log-normalized SW density, slope, and amplitude were assessed with ANOVAs using age and derivations as fixed factors. Contrast analyses were performed when significant interactions were found and appropriate effect size measures were computed. Results were considered significant when $p < 0.05$. For the mediation analyses, we also report unstandardized regression coefficients of age effect on SW characteristics (density, amplitude, and slope) at each derivation, as printed by PROCESS (path c).

Step 2: Relationship between CT and SWs when controlling for the effects of age (path b only)

Statistical models predicting CT were constructed using SurfStat (http://www.math.mcgill.ca/keith/surfstat/) on MATLAB 2011a for Mac. In the first stage, models included fixed factors related to the SW characteristic of interest in each analysis (density, amplitude, or slope), but also to age group, sex, and intracranial volume (ICV). Preliminary analyses also included an interaction term between age group and SW characteristics to ensure that the relationship between SWs and CT did not differ significantly between younger and older adults. We used an uncorrected threshold of $F_{(1,57)} = 12.04$ ($p < 0.001_{\text{uncorrected}}$) to identify clusters of vertices where we could find an interaction between age and whole-night SW characteristics. Because no significant interactions between SW characteristics and age group were found, we dropped the interaction term from subsequent models. Therefore, the final models included fixed factors related to the SW characteristic of interest (density, amplitude, or slope), as well as age group, ICV, and sex as covariables. We used a threshold of $T_{(58)} = 3.24$ ($p < 0.001_{\text{uncorrected}}$) to test the main effects of SWs. Results were corrected for multiple comparisons ($p < 0.05_{\text{whole-brain}}$) using random-field theory (RFT; Worsley et al., 2004).

Step 3: Effects of age on regions linked to SWs (path a only)

Conjunction analyses were performed to identify regions that were jointly related to both SW characteristics at each derivation and age group. This two-stage analysis allowed for the isolation of CT regions that not only presented significant age-related thinning, but were also significantly associated with SW characteristics when controlling for age.

Table 1. PSG variables

	Young adults ($n = 30$)	Older adults ($n = 33$)	Age effect (p-value)
Sleep duration (min)	451.3 (6.6)	397.2 (8.7)	$p < 0.001$
Sleep efficiency (%)	93.11 (5.6)	83.9 (9.7)	$p < 0.001$
N1 (min)	33.78 (16.5)	42.72 (19.0)	$p = 0.05$
N2 (min)	239.1 (34.0)	239.0 (38.1)	NS
N3 (min)	84.6 (25.7)	40.2 (30.1)	$p < 0.001$
REM (min)	93.8 (26.3)	75.3 (24.5)	$p = 0.005$
N3 (%)	18.8 (5.9)	10.1 (7.5)	$p < 0.001$

Mean values for sleep variables are displayed along with the associated SDs for both age groups. p-values are based on t test corrected for unequal variance between groups.

To do this, we first computed an independent age effect map on CT (ICV and sex included as covariables; minimal $T_{(59)} = 3.23$, $p < 0.001_{\text{uncorrected}}$) and corrected results at $p < 0.05$ with RFT. Second, we isolated intersecting CT clusters between this last contrast and the effect map of SW characteristics corrected at $p < 0.05$ (RFT) (see Step 2 above). This ensured that regions in conjunction were significant for both the age effect and the SW effect (while correcting for age) with a minimal threshold on the corrected p-value of $p = 0.05$.

*Step 4: Simple mediation modeling (test of indirect effects; path a*path b)*

To quantify how changes in each CT cluster identified in step 3 (conjunction analyses) were involved in age-related changes in SWs, we performed simple mediation analyses. For each cluster, we first calculated mean CT corrected for ICV and then entered mean CT in each cluster independently as a mediator in several simple mediation models explaining age-related effects on SW characteristics by changes in CT. Indirect effects were considered significant ($p < 0.05$) when the 95% confidence interval (95% CI) of the bootstrapped coefficient (5000 bootstrap iterations) did not include zero. We also computed mediation effect sizes (K^2) for each region.

Step 5: Integrative modeling

As a means to evaluate which CT clusters identified in Step 3 explained age-related changes in SW characteristics when controlling for the other CT clusters, we performed a parallel mediation analysis for each SW characteristic (Hayes, 2013). This analysis computed the significance of indirect effects associated with each region of interest while they were in competition as mediators within the same model. We also computed significance of contrasts between significant indirect effects.

Results

Step 1: Effects of age on sleep parameters and all-night SW characteristics in frontal regions (path c only)

Age differences in global PSG variables are described in Table 1. Previous studies reported the preeminence of an age effect on SW characteristics in frontal derivations (Landolt and Borbély, 2001; Carrier et al., 2011; Lafortune et al., 2012). We replicated these results in the present study, as age effect sizes were found to be preeminent in frontal regions (Fig. 2). In frontal regions, older subjects showed lower SW density ($b = -0.34$, $p < 0.001$), amplitude ($b = -0.08$, $p < 0.001$), and slope ($b = -0.14$, $p < 0.001$) (Table 2). These unstandardized betas were entered in subsequent mediation modeling analyses.

Step 2: Relationship between CT and whole-night SW characteristics in frontal derivations when controlling for the effects of age (path b only)

Higher frontal SW density was significantly associated with higher CT in a large cluster within the right superior temporal lobe (R.STL). Moreover, higher frontal SW density was also significantly associated with higher CT in three additional restrained clusters (Fig. 3*A*, Table 3), one located in the right inferior parietal lobule (R.IFP), in its supramarginal portion

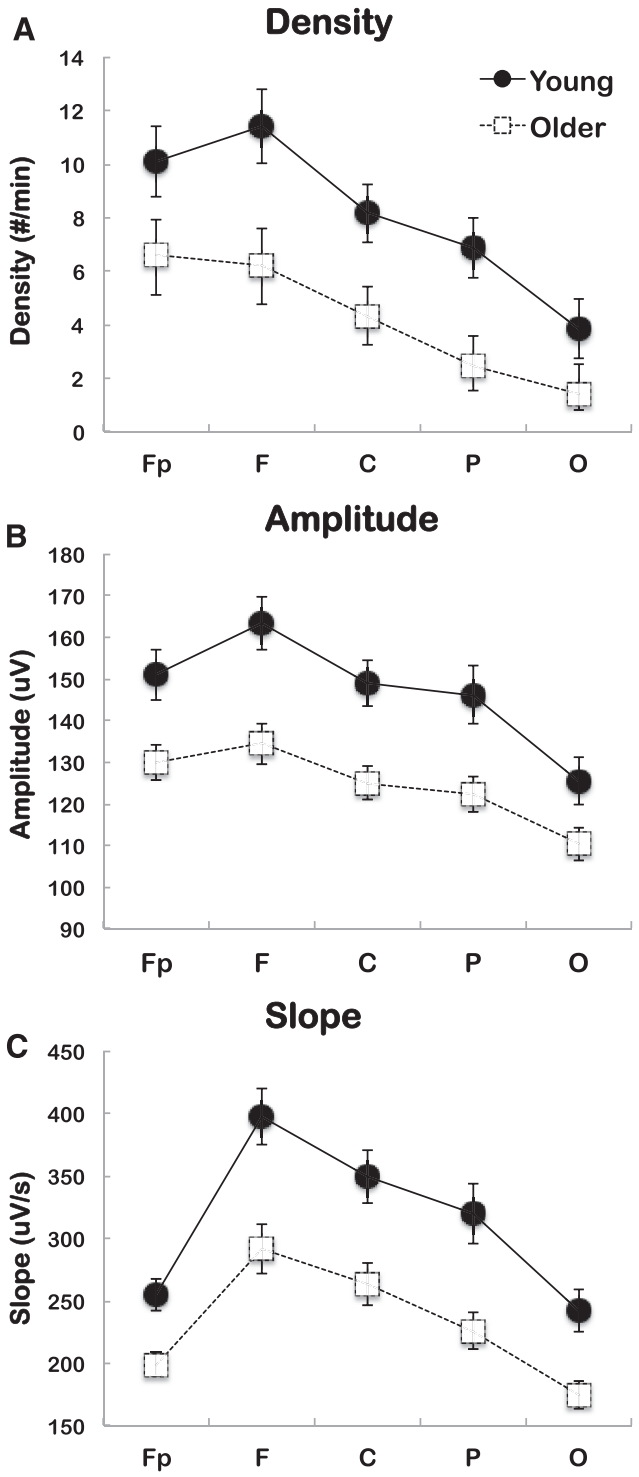

Figure 2. SW characteristics showing significant interaction between derivations and age group. SW density (top), SW amplitude (middle), and SW slope (bottom) are shown for young subjects (black dots) and older subjects (open squares). ***A***, Older subjects show lower SW density in every derivation (contrast analysis, $*p < 0.001$), but effect size measures indicate a predominant effect of age in frontal (F) derivations. Effect sizes: $F_p = 0.205$, $F = 0.315$, $C = 0.305$, P = 0.266, $O = 0.239$). ***B***, Older subjects show lower SW amplitude in all derivations (contrast analysis, $*p < 0.001$), but effect size measures show preeminent effects in frontal (F) derivations. Effect sizes: $F_p = 0.352$, $F = 0.462$, $C = 0.453$, P = 0.393, $O = 0.245$. ***C***, Older subjects show decreased SW slope in all derivations (contrast analysis, $*p < 0.001$), but effect size measures indicate a predominant effect of age in frontal (F) derivations. Effect sizes: $F_p = 0.465$, $F = 0.473$, $C = 0.406$, P = 0.464, $O = 0.435$. Effect size index $= \eta^2$.

Table 2. SW variables in frontal derivations

	Young adults ($n = 30$)	Older adults ($n = 33$)	Age effect (p value)
SW density (nb/min)	11.41 (3.90)	6.23 (4.32)	$p < 0.001$
SW amplitude (μV)	163.33 (18.03)	134.49 (14.60)	$p < 0.001$
SW slope (μV/s)	397.67 (62.78)	291.22 (58.05)	$p < 0.001$

Mean values for raw frontal SW variables are displayed along with associated SDs for both age groups. Log-normalized data have been analyzed and used in subsequent analyses. p-values are based on t test corrected for unequal variance between groups.

(BA40), another in the middle frontal gyrus (R. MFG; BA6), and a last cluster in the middle temporal and inferotemporal gyri (BA20/BA21). The large cluster in the R.STL included regions from the primary auditory cortex, the superior temporal gyrus, the transverse gyrus (BA41), and the insula (BA13). There were no negative significant relationships between CT and SW density.

Higher SW amplitude in frontal derivations was associated with higher CT in a large cluster in the right superior parietal lobule (R.SPL; BA7). Moreover, higher SW amplitude was associated with a more delimited region in the R.MFG (BA6), and two regions in the left occipital lobe, in its extrastriate and associative portions, near the left cuneus (BA19) and lingual gyrus (BA18) (Fig. 3*B*, Table 3). The large cluster, defined as the right superior parietal lobe, included the border of the precuneus (BA7) and most of the R.SPL (BA7). There were no negative significant relationships between CT and SW amplitude.

SW slope in frontal derivations was not associated with CT in any cluster, whether in positive or negative contrasts ($p < 0.05$ corrected; Table 3). Therefore, we did not further investigate the role of cortical thinning in age-related reduction of frontal SW slope.

Step 3: Effects of age on regions linked to frontal SW density and amplitude (path a only)

Conjunction analyses were performed to isolate cortical regions associated with frontal SW characteristics (while controlling for age; path b) and also linked to age (path a) (Table 4).

Most regions that were related to frontal SW density (when controlling for age) also showed significant age-related thinning (Fig. 4). All vertices in the R.STL, MFG, and IPL clusters showed age-related differences between young and older adults (Table 4). However, 59 vertices (of 89) in the superior boundary of the right middle temporal gyrus cluster were thinner in older subjects: those that survived were mainly located in the right inferotemporal gyri (ITG) and right middle temporal gyri.

All vertices associated with SW amplitude located in the right SPL and MFG showed age-related thinning in older adults (Fig. 5). However, only the medial portion of the left cuneus cluster was affected by age (71 of 289 vertices showed significant age-related effects).

Step 4: Simple mediations in frontal derivations (test of indirect effects; path a *path b)

For mediation to occur, we must demonstrate that including the mediator (in this case, CT in specific areas associated with SW density or amplitude in frontal derivations) does attenuate the effect of age in a model in which age predicts SW density or SW amplitude in frontal derivations (significant indirect effect).

Independent tests of indirect effects in frontal derivations (one mediator by analysis) are depicted in Table 5 for frontal SW density and in Table 6 for frontal SW amplitude. In these tables, path c represents the initial total effect of age on each frontal SW characteristic when CT is not included in the model. Changes in explained variance when adding CT to age in models predicting frontal SW density (path c) is also reported. Parameter estimates of path a represent the size and significance of age effects on CT. Path b

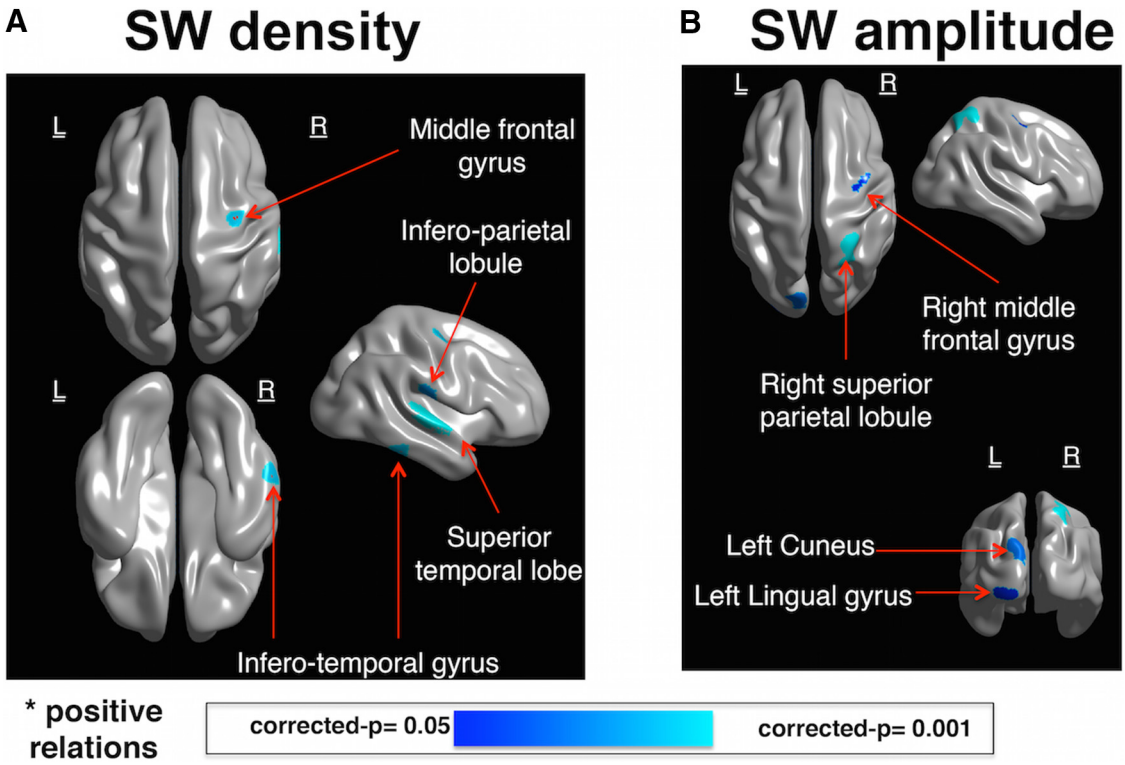

Figure 3. Main effects of frontal SW density (***A***) and frontal SW amplitude (***B***) on CT. Models included effects of age group, sex, and ICV. Effects are displayed on an average surface constructed from mesh derived from the CIVET pipeline. Images from both age groups were normalized to the MNI space before calculating contrasts ($p < 0.001_{\text{uncorrected}}$ and then corrected using random-fields theory at $p < 0.05_{\text{whole-brain}}$). Colors display *p*-value. Dark blue is $p = 0.05_{\text{whole-brain}}$; light blue is $p = 0.001_{\text{whole-brain}}$.

Table 3. Positive associations between SW characteristics and CT

Region (BA)	Cluster size (vertices)*	Corresponding *p* value*	Coordinates of peak (MNI space)
SW density and CT			
Right superior temporal lobe (BA41/BA22/BA13)	631	$p < 0.001$	(60 −19 0)
Right middle frontal gyrus (BA6)	68	$p = 0.008$	(35 −9 57)
Right middle/inferior temporal gyri (BA21/BA20)	89	$p = 0.009$	(58 −37 −19)
Right inferoparietal lobule (BA40)	111	$p = 0.02$	(56 −20 22)
SW amplitude and CT			
Right superior parietal lobe (BA7)	356	$p < 0.001$	(27 −48 65)
Left cuneus (BA19)	289	$p = 0.02$	(−7 −88 30)
Right middle frontal gyrus (BA6)	62	$p = 0.04$	(37 −6 55)
Left lingual gyrus (BA18)	139	$p = 0.04$	(−23 −97 −8)

Cluster results of whole-brain analyses of positive contrast between frontal SW density and frontal SW amplitude with CT. Results include sex, ICV, and age group as covariables and are corrected at $p < 0.05_{\text{whole-brain}}$ with random fields.

*Coordinates of peaks for each significant cluster in relevant contrast are displayed.

represents the relationship between CT and frontal SW characteristics when the effects of age are controlled for. Path c′ represents the residual effects of age group on frontal SW characteristics when CT is included in the model. The last column reflects the significance of the indirect effects of age mediated by CT and their associated effect sizes (the ratio of the obtained indirect effect to the maximum possible indirect effect; Preacher and Kelley, 2011).

Whereas age group initially explained 32% of the variance in frontal SW density, adding CT regions to the models resulted in an increase of the amount of explained variance in frontal SW density by 14–23% (depending of the region). In addition, whereas age group alone initially explained 46% of the variance in frontal SW amplitude, the level of explained variance increased between 9% and 11% when adding CT measures to the models. Inspection of simple mediation models showed that thinning in each region consistently and significantly attenuated the effect of age (direct/total effect) on frontal SW density and amplitude (indirect effects column, Tables 5, 6). For frontal SW density, indirect effects were significant in every region, but were strongest in the right MFG ($K^2 = 0.35$) and right STL ($K^2 = 0.32$), and moderate in the right ITG ($K^2 = 0.22$) and IPL ($K^2 = 0.23$). Most importantly, after accounting for CT in the right MFG or right STL, there was no residual direct effect of age on frontal SW density ($p = 0.22$; path c′).

For frontal SW amplitude, indirect effects of age were significant in all regions, but were strongest in the right MFG ($K^2 = 0.29$) and right SPL ($K^2 = 0.27$) and moderate in the left cuneus ($K^2 = 0.18$). After accounting for CT in all of these regions, there was still a residual direct effect (path c′) of age on frontal SW amplitude ($p < 0.05$).

Step 5: Integrative modeling

SW density in frontal derivations

Simultaneously entering age and CT of the right MFG, STL, ITG, and IPL in a model predicting frontal SW density increased the explained variance by 33% compared with the initial model (path c) on SW density (model 2 vs model 1, Table 7). As previous analyses showed, the increase in variance in individual models was between 14% and 23%. Therefore, this last analysis indicates additional properties of CT in different regions, which helped to predict frontal SW density. In this integrative model, there were independent and specific indirect effects of age mediated by changes in CT in the right ITG and MFG (model 2, Table 7), but not in the other two cortical areas. Contrast between these two indirect effects was not significant ($b = 0.03$, 95% CI: [−0.13

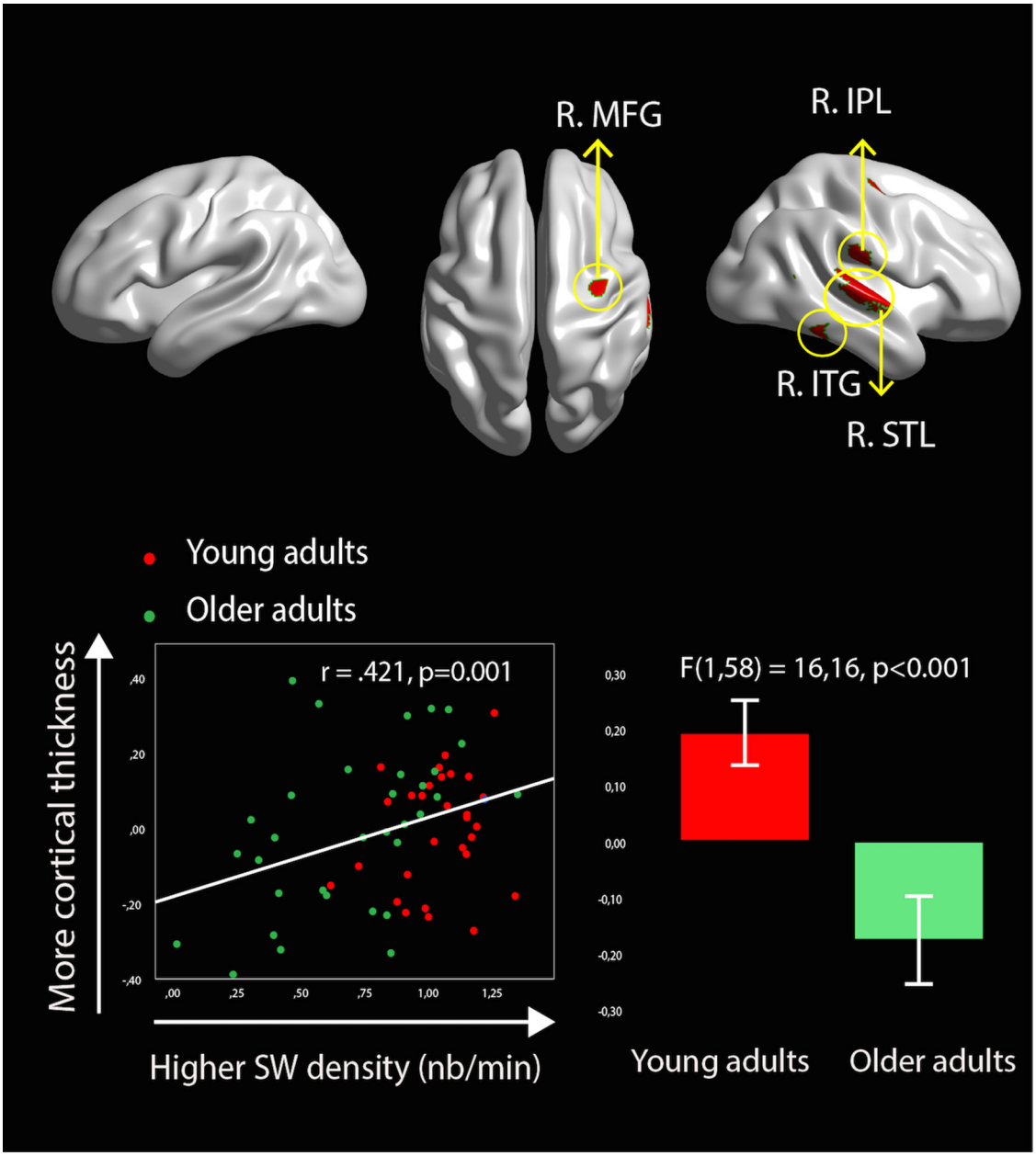

Figure 4. Variations in CT are associated with individual differences in both age and frontal SW density. Brain images show the results of the conjunction analysis in which CT is negatively associated with age independently of sex and ICV ($p < 0.05$, corrected) and positively associated with frontal SW density independently of age, sex, and ICV ($p < 0.05$, corrected). A typical example is shown on the lower side of the figure. The scatterplot at the bottom left corner displays the relationship between residuals of log-normalized frontal SW density and residuals of mean CT (controlled for ICV, sex, and age) in the right SPL. The boxplot in the bottom right corner shows the age effect on residuals of CT in the right SPL (controlling for ICV and sex).

Table 4. Conjunction analysis: effect of age and SW characteristics on CT

Region (BA)	Cluster size (vertices)	Coordinates of peak (MNI space)
SW density		
Right superior lobe (BA41/BA22/BA13)	631	(60 −19 0)
Right middle frontal gyrus (BA6)	68	(35 −9 57)
Right middle/inferior temporal gyri (BA21/BA20)	59	(58 −37 −19)
Right inferoparietal lobule (BA40)	111	(56 −20 22)
SW amplitude		
Right superior parietal lobe (BA7)	356	(27 −48 65)
Left cuneus (BA19)	71	(−12 −88 33)
Right middle frontal gyrus (BA6)	62	(37 −6 55)

Regions showing both significant frontal SW effects ($p < 0.05$ RFT-corrected, correcting for age, sex, and whole brain volume) and age effects ($p < 0.05$ RFT-corrected, correcting for sex and whole brain volume). Peak coordinates of SW effects in each conjunct-related cluster are displayed.

0.21]), meaning that age-related changes in frontal SW density seem to involve thinning of similar amplitude in these two regions. Importantly, aging did not present any residual direct effect on frontal SW density in this model.

SW amplitude

Here, we examined the roles of thinning of the right MFG, SPL, and left cuneus in the decline of frontal SW amplitude. Simultaneously entering the above-mentioned regions of interest (in significant conjunction), in addition to age, into a model predicting frontal SW amplitude resulted in a 13% increase in explained variance compared with the initial model containing only the total effects of age (path c) (model 2 vs model 1, Table 8). Computation of indirect effects showed that inclusion of CT in all regions into the model explained a significant part of the age-

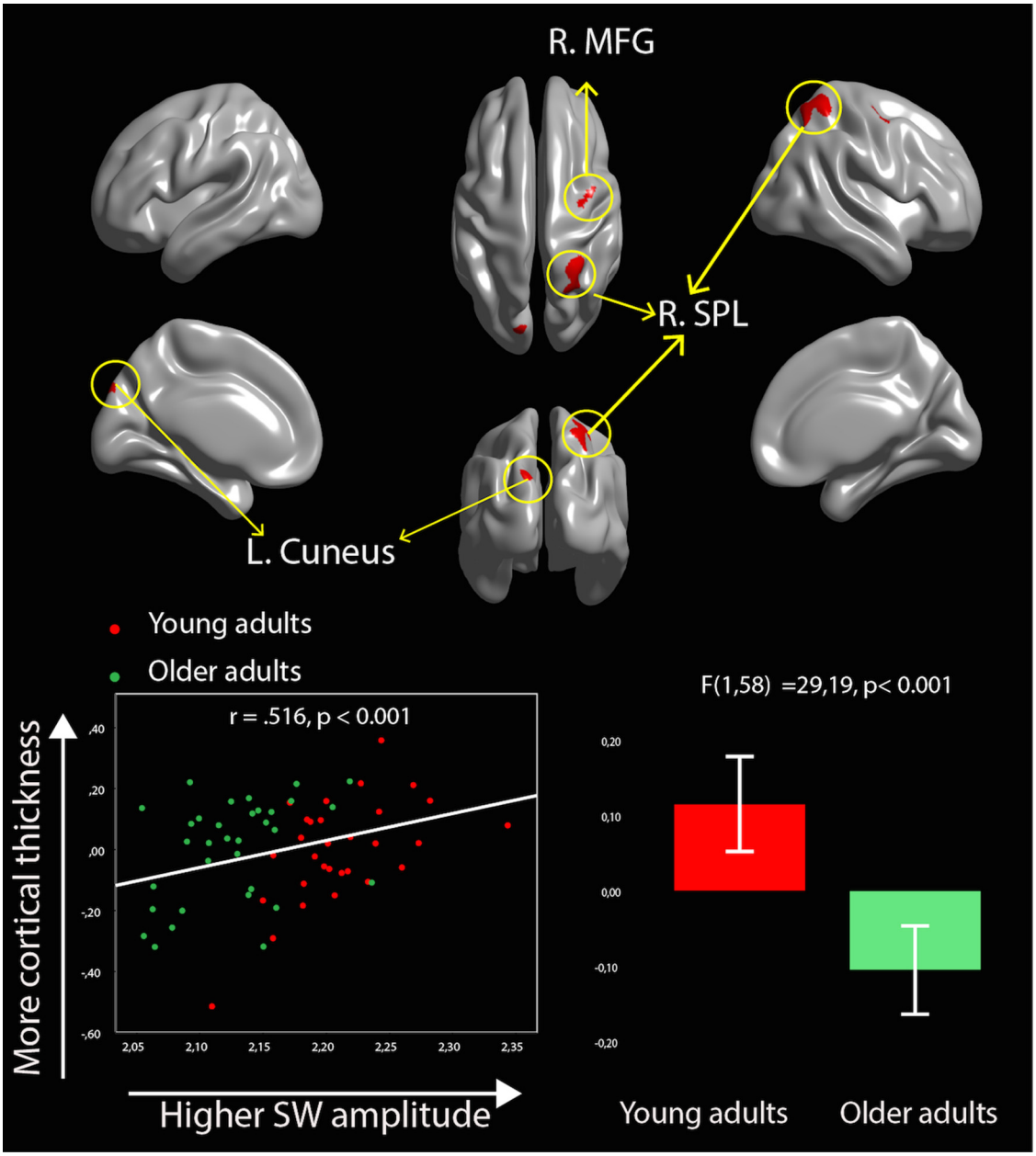

Figure 5. Variations in CT are associated with individual differences in both age and frontal SW amplitude. Brain images show the results of the conjunction analysis in which CT is negatively associated with age independently of sex and ICV ($p < 0.05$, corrected) and positively associated with frontal SW amplitude independently of age, sex, and ICV ($p < 0.05$, corrected). A typical example is shown on the lower side of the figure. The scatterplot at the bottom left corner displays the relationship between residuals of log-normalized frontal SW amplitude and residuals of mean CT (controlled for ICV, sex, and age) in the right MFG. The boxplot in the bottom right corner shows the age effect on residuals of mean CT in the right MFG (controlling for ICV and sex).

Table 5. Simple mediation results for SW density in frontal derivations

Path c (total effect of age on frontal SW density): $b = -0.34$, $R^2 = 0.32$, $p < 0.001$

Region	Lat	BA	Size	Change in variance compared with path c ($\delta F_{(df)}$, δR^2, p value)	Parameter estimates: Path a	Path b	Path c′	Indirect effect (b, 95% CI, K^2)
STL	R	41/22/13	631	$\delta F_{(1,60)} = 21.3$, $\delta R^2 = 0.18$, $p < 0.001$	$b = -0.30$, $p < 0.001$	$b = 0.68$, $p = 0.001$	$b = -0.13$, $p = 0.06$	$b = -0.20$ (−0.32 −0.11) (*) $K^2 = 0.32$
MFG	R	6	68	$\delta F_{(1,60)} = 19.8$, $\delta R^2 = 0.17$, $p < 0.001$	$b = -0.37$, $p < 0.001$	$b = 0.65$, $p < 0.001$	$b = -0.10$, $p = 0.22$	$b = -0.24$ (−0.40 −0.11) (*) $K^2 = 0.35$
ITG	R	21/22	59	$\delta F_{(1,60)} = 30.8$, $\delta R^2 = 0.23$, $p < 0.001$	$b = -0.24$, $p < 0.001$	$b = 0.69$, $p < 0.001$	$b = -0.17$, $p = 0.005$	$b = -0.16$ (−0.27 −0.08) (*) $K^2 = 0.29$
IPL	R	40	111	$\delta F_{(1,60)} = 15.9$, $\delta R^2 = 0.14$, $p < 0.001$	$b = -0.21$, $p < 0.001$	$b = 0.73$, $p < 0.001$	$b = -0.19$, $p = 0.008$	$b = -0.15$ (−0.25 −0.07) (*) $K^2 = 0.25$

Rows illustrate the simple mediation model for frontal SW density with mean CT in each region as stand-alone mediators. δF indicates the change in explained variance due to inclusion of the CT cluster as a mediator compared with the total effect model (path c). Coefficients in each path necessary for the computation of indirect effects are shown in designated columns. b-values refer to unstandardized parameter estimates of paths shown in Figure 1. Indirect effects are significant at $p < 0.05$ when 0 is not included in the 95% CI; and significance is denoted with an asterisk. K^2 is an effect size of mediation and thus represents the proportion of the age-related effect on frontal SW density that has been mediated by changes in CT (>0.25 = strong effect; >0.09 = medium effect; >0.001 = small effect). CT in each region is adjusted for ICV.

Table 6. Simple mediation results for SW amplitude in frontal derivations

Path c (total effect of age): $b = -0.08$, $R^2 = 0.46$, $p < 0.001$

Region	Lat	BA	Size	Change in variance compared with path c ($\delta F_{(df)}$, δR^2, p value)	Parameter estimates			
					Path a	Path b	Path c′	Indirect effects (b, 95% CI, K^2)
SPL	R	7	356	$\delta F_{(1,60)} = 15.6$, $\delta R^2 = 0.11$, $p < 0.001$	$b = -0.22$, $p < 0.001$	$b = 0.13$, $p < 0.001$	$b = -0.06$, $p < 0.001$	$b = -0.03$ (−0.05 −0.01) (*) $K^2 = 0.25$
Cuneus	L	19	71	$\delta F_{(1,60)} = 11.7$, $\delta R^2 = 0.09$, $p = 0.001$	$b = -0.16$, $p < 0.001$	$b = 0.11$, $p = 0.001$	$b = -0.07$, $p < 0.001$	$b = -0.02$ (−0.03 −0.01) (*) $K^2 = 0.17$
MFG	R	6	68	$\delta F_{(1,60)} = 11.4$, $\delta R^2 = 0.09$, $p = 0.001$	$b = -0.33$, $p < 0.001$	$b = 0.11$, $p = 0.001$	$b = -0.05$, $p = 0.003$	$b = -0.04$ (−0.06 −0.02) (*) $K^2 = 0.28$

Rows illustrate simple mediation models for frontal SW amplitude with mean CT in each region as stand-alone mediators. δF indicates the change in explained variance due to inclusion of the CT cluster as a mediator compared with the total effect model (path c). Coefficients in each path necessary for the computation of indirect effects are shown in designated columns. b-values refer to unstandardized parameters estimates of paths shown in Figure 1. Indirect effects are significant at $p < 0.05$ when 0 is not included in the 95% CI and significance is denoted with an asterisk. K^2 is an effect size of mediation and thus represents the proportion of the age-related effect on frontal SW amplitude that has been mediated by changes in CT (>0.25 = strong effect; >0.09 = medium effect; >0.001 = small effect). CT in each region is adjusted for ICV.

Table 7. Parallel mediation results (SW density in frontal derivations)

Effects	Significance of effects (b, p-value, or 95% CI)	Change in variance between models ($\delta F_{(df)}$, δR^2, p value)
Model 1 (initial model)		$\delta F_{(1,61)} = 28.06$, $\delta R^2 = 0.32$, $p < 0.001$
Total effect of age on SW density$_{(path\ c)}$	$b = -0.34$, $p < 0.001$	
Model 2 (parallel mediation model)		$\delta F_{(4,57)} = 13.53$, $\delta R^2 = 0.33$, $p_{(\delta F)} = 0.001$
Direct effect of age on SW density$_{(path\ c')}$	$b = -0.001$, $p = 0.99$	
Total indirect effect of age on SW density mediated by changes in CT$_{(path\ a \times path\ b)}$	$b = -0.34$, (−0.47 −0.22) (*)	
Specific indirect effects of age on SW density (in model 2) through		
Changes in IFP$_{(path\ a \times path\ b)}$	$b = 0.01$, (−0.07 0.10), NS	
Changes in ITG$_{(path\ a \times path\ b)}$	$b = -0.12$, (−0.21 −0.05) (*)	
Changes in MFG$_{(path\ a \times path\ b)}$	$b = -0.13$, (−0.28 −0.01) (*)	
Changes in STL$_{(path\ a \times path\ b)}$	$b = -0.10$, (−0.23 0.01), NS	

Total effects of age on frontal SW density in the initial model (path c; model 1) compared with indirect and residual (direct) effects of age on frontal SW density in a parallel mediation model (model 2). δF and δR^2 for model 1 refer to the variance explained by the age-only model compared with a constant, whereas values for model 2 refer to variance explained in model 2 (parallel mediation by CT) compared with variance explained in model 1. Individual coefficients in each path for each mediator are not shown; only significance for indirect effects are shown. Note that path a coefficients are the same as in Table 5, whereas path b coefficients are adjusted in the model when all mediators are included simultaneously. Indirect effects are tested, significance is attained at $p < 0.05$ when 0 is not included in the 95% CI and significance is denoted with an asterisk. CT is adjusted for these models.

Table 8. Parallel mediation results (SW amplitude in frontal derivations)

Effects	Significance of effects (b, p-value, or 95% CI)	Change in variance between models ($\delta F_{(df)}$, δR^2, p)
Model 1 (initial model)		$\delta F_{(1,61)} = 52.34$, $\delta R^2 = 0.46$, $p < 0.001$
Total effect of age on SW amplitude$_{(path\ c)}$	$b = -0.08$, $p < 0.001$	
Model 2 (parallel mediation model)		$\delta F_{(4,57)} = 6.43$, $\delta R^2 = 0.13$, $p_{(\delta F)} = 0.001$
Direct effect of age on SW amplitude $_{(path\ c')}$	$b = -0.05$, $p = 0.002$	
Total indirect effect of age on SW amplitude, mediated by changes in CT$_{(path\ a \times path\ b)}$	$b = -0.04$, (−0.06 −0.02) (*)	
Specific indirect effects of age (in model 2) on SW amplitude mediated by		
Changes in SPL$_{(path\ a \times path\ b)}$	$b = -0.01$, (−0.04 0.01), NS	
Changes in cuneus$_{(path\ a \times path\ b)}$	$b = -0.01$, (−0.03 0.01), NS	
Changes in MFG$_{(path\ a \times path\ b)}$	$b = -0.02$, (−0.04 0.01), NS	

Total effects of age on frontal SW amplitude in the initial model (model 1; path c) compared with indirect and residual (direct) effects of age on frontal SW amplitude in a parallel mediation model (model 2). δF and δR^2 for model 1 refer to the variance explained by the age-only model compared with a constant, while values for model 2 refer to variance explained in model 2 (parallel mediation by CT) compared with variance explained in model 1. Individual coefficients in each path, for each mediator, are not shown; only significance for indirect effects are shown. Note that path a coefficients are the same as in Table 6, whereas path b coefficients are adjusted in the model when all mediators are included simultaneously. Indirect effects are significant at $p < 0.05$ when 0 is not included in the 95% CI and significance is denoted with an asterisk. CT is adjusted for ICV in these models.

related decrease of frontal SW amplitude. However, there was still a significant residual direct effect of age on frontal SW amplitude. Moreover, no region presented significant specific indirect effects, indicating that focal thinning of one of these regions could not by itself explain the age-related decrease of frontal SW amplitude. Instead, overall thinning in all of these regions could explain some part of the age-related decrease in SW amplitude (Table 8).

Relationships between CT and SW characteristics in other derivations

SW density

We also investigated associations between CT and SW characteristics in the prefrontal, central, parietal, and occipital derivations when controlling for the effects of age. Higher SW density in prefrontal, central, and parietal derivations, but not in occipital derivations, was associated with higher CT in several regions (Table 9). Higher prefrontal SW density was associated with higher CT in an inferoparietal cluster comprising the ventral part of the postcentral gyrus and the supramarginal gyrus located dorsally to the posterior part of the lateral fissure (BA40/BA43). Furthermore, higher central SW density was associated with higher CT in a large cluster that included the insula (BA13) and part of the superior temporal area (BA22) and another cluster in the middle frontal gyrus (BA6). In addition, higher parietal SW density was associated with higher CT in both the insula (BA13) and middle cingulate cortices (BA24). There were no negative significant relationships between CT and SW density in any derivation.

All cortical regions associated with SW density in prefrontal, central, and parietal derivations (except the cingulate cortex) were thinner in older subjects (conjunct vertices column, Table 9). Moreover, for each of these regions, cortical thinning explained a significant proportion of the age-related decrease of SW density (indirect effects column, Table 9). Because there were significant indirect effects of age on central SW density mediated by changes in the right insula and the right middle frontal regions, an independent parallel mediation analysis was applied to determine which of these two regions drives the age-related de-

Table 9. Topological association between CT and SW density and related mediation analysis

Total effect of age at each derivation (path c) (*b*, *p*-value)	CT cluster (BAs, peak)	Lat	Cluster size (corrected *p* value)	Conjunct vertices (age and SW)	Parameter estimates (simple mediation models) Path a	Path b	Path c′	Indirect effect (*b*, 95% CI, K^2)
Prefrontal	IFP (BA40/BA43)	R	85 vertices	85	$b = -0.20$,	$b = 0.74$,	$b = -0.10$,	$b = -0.15$ (−0.25 −0.06) (*) $K^2 = 0.26$
$b = -0.25$, ($p = 0.002$)	(56 −18 20)		$p = 0.05$		$p < 0.001$	$p < 0.001$	$p = 0.14$	
Central	Insula (BA13/BA22)	R	171 vertices	171	$b = -0.30$,	$b = 0.55$,	$b = -0.20$,	$b = -0.17$ (−0.29 −0.07) (*) $K^2 = 0.25$
$b = -0.36$, ($p < 0.001$)	(46 −1 −10)		$p = 0.002$		$p < 0.001$	$p < 0.001$	$p = 0.01$	
	MFG	R	42 vertices	42	$b = -0.37$,	$b = 0.68$,	$b = -0.11$,	$b = -0.25$ (−0.43 −0.11) (*) $K^2 = 0.33$
	(BA6) (30 −10 59)		$p = 0.05$		$p < 0.001$	$p < 0.001$	$p = 0.18$	
Parietal	Insula (BA13)	R	119 vertices	119	$b = -0.30$,	$b = 0.70$,	$b = -0.21$,	$b = -0.21$ (−0.44 −0.08) (*) $K^2 = 0.25$
$b = -0.42$, ($p < 0.001$)	(46 −1 −10)		$p = 0.007$		$p < 0.001$	$p < 0.001$	$p = 0.04$	
	Middle cingulate (BA24)	R	46 vertices	46	NA	NA	NA	NA
	(2 −3 26)		$p = 0.009$					

Rows illustrate simple mediation models to explain age-related changes in SW density at other derivations (prefrontal, central, parietal, and occipital) with mean CT in each previously identified region as stand-alone mediators. Total effect of age on SW density is shown under each derivation. The cluster column depicts the relationship between cluster and SW density when controlling for age. The conjunction analysis column depicts the number of vertices also significantly associated with age-related thinning. Coefficients in each path necessary for the computation of indirect effects are shown in designated columns. *b*-values refer to unstandardized parameter estimates of paths shown in Figure 1. Indirect effects are significant at $p < 0.05$ when 0 is not included in the 95% CI and significance is denoted with an asterisk. K^2 is an effect size of mediation and thus represents the proportion of the age-related effect on SW density that has been mediated by changes in CT (>0.25 = strong effect; >0.09 = medium effect; >0.001 = small effect). CT in each region is adjusted for ICV.

Table 10. Topological association between CT and SW amplitude and related mediation analyses

Total effect of age at each derivation (path c) (*b*, *p*-value)	CT cluster (BAs, peak)	Lat	Cluster size (corrected *p* value)	Conjunct vertices (age and SW)	Parameter estimates (simple mediation models) Path a	Path b	Path c′	Indirect effect (*b*, 95% CI, K^2)
Prefrontal	Cuneus (BA19)	L	322 vertices	55	$b = -0.17$,	$b = 0.12$,	$b = -0.04$,	$b = -0.02$ (−0.04 −0.01) (*) $K^2 = 0.21$
$b = -0.06$, $p < 0.001$	(−14 −89 33)		$p = 0.009$		$p < 0.001$	$p < 0.001$	$p < 0.001$	
Parietal	MPFC (BA9)	L	456 vertices	84	$b = -0.23$,	$b = 0.11$,	$b = -0.05$,	$b = -0.02$ (−0.05 −0.01) (*) $K^2 = 0.22$
$b = -0.08$, $p < 0.001$	(−6 48 29)		$p = 0.02$		$p < 0.001$	$p < 0.001$	$p < 0.001$	

Rows illustrate simple mediation models to explain age-related effects on SW amplitude at other derivations (prefrontal, central, parietal, and occipital) with mean CT in each previously identified region as stand-alone mediators. The cluster column depicts the relationship between cluster and SW amplitude at different electrodes when controlling for age. Total effect of age on SW amplitude is shown under each derivation. The conjunction analysis column depicts the number of vertices also significantly associated with age-related thinning. Coefficients in each path necessary for the computation of indirect effects are shown in designated columns. *b*-values refer to unstandardized parameter estimates of paths shown in Figure 1. Indirect effects are significant at $p < 0.05$ when 0 is not included in the 95% CI and significance is denoted with an asterisk. K^2 is an effect size of mediation and thus represents the proportion of the age-related effect on SW amplitude that has been mediated by changes in cortical thickness (>0.25 = strong effect; >0.09 = medium effect; >0.001 = small effect). CT in each region is adjusted for ICV.

crease of central SW density. The model (not shown in the tables) reveals two significant specific indirect effects: $b_{\text{frontal}} = -0.19$ (95% CI = −0.35 −0.06) and $b_{\text{insula}} = -0.11$ (95% CI = −0.21 −0.03). There were no residual direct effects (path c′) of age on central SW density in this model ($b = -0.06$, $p = 0.46$). Therefore, thinning of both middle frontal and insular cortices accounts for the age-related decrease in central SW density.

SW amplitude

Higher SW amplitude in prefrontal, central, and parietal derivations, but not in occipital derivations, was associated with higher CT in different cortical areas when controlling for the effects of age (Table 10). Higher prefrontal SW amplitude was associated with higher CT in occipital extrastriate cortex near the cuneus (BA19), whereas higher parietal SW amplitude was associated with higher CT in the medial prefrontal cortex (BA9). A trend was also observed for central SWs, for which higher amplitude was associated with higher CT in the right superior parietal lobe (corrected *p*-value: 0.059; 106 vertices; nearest peak: 28 −48 65, BA7). There were no negative significant relationships between CT and SW amplitude in any derivation.

The medial prefrontal cortex, the cuneus cortex, and the superior parietal lobe (which was nearly significantly associated with SW amplitude in central derivations in the last analysis) were thinner in older subjects (conjunct vertices column, Table 10; SPL is not shown in the tables because this result is only near significance). Significant indirect effects were also observed in all regions.

There were no negative or positive significant relationships between CT and SW slope in any derivation.

Age-related changes in SW characteristics during the first NREM period

Because age-related differences in SWs are more prominent at the beginning of the night (Carrier et al., 2011), we investigated the role of cortical thinning in age-related changes in frontal SW characteristics in the first NREMP. Results presented in Tables 11 and 12 indicate that higher frontal SW density and amplitude for the first NREMP were associated with higher CT (when controlling for age) in various areas. Higher frontal SW density in the first NREMP was associated with higher CT in the right MFG and the right ITG, whereas higher frontal SW amplitude was associated with higher CT in right MFG, right SPL, left cuneus, and left IFP. There were no significant negative contrasts between CT and frontal SW density or frontal SW amplitude during the first NREMP. Frontal SW slope in the first NREMP was not associated with CT in either negative or positive contrasts. Older subjects showed thinner cortex in all regions associated with frontal SW density and amplitude in the first NREMP (conjunct vertices column, Tables 11, 12). Furthermore, there were significant indirect effects in all of these cortical regions, indicating that cortical thinning significantly explained the age-related decrease of frontal SW density and amplitude during the first NREMP (indirect effects column, Tables 11, 12).

Table 13 shows the results for the parallel mediation analyses for frontal SW density in first NREMP. Simultaneously entering age and right IT and MFG CT in a model predicting frontal SW density during the first NREMP enhanced explained variance by 21% compared with the initial model containing only the total effects of age (path c, model 2 vs model 1, Table 13). Total ex-

Table 11. Association between CT and frontal SW density in the first NREMP and related mediation analyses

Total effect of age on frontal SW density in the first sleep NREMP (path c): -0.41, $p < 0.001$							
CT cluster (BAs, peak)	Lat	Cluster size (corrected p-value)	Conjunct vertices (age and SW)	Parameter estimates (simple mediation models) Path a	Path b	Path c′	Indirect effect (b, 95% CI, K^2)
ITG BA21 (59 −38 −19)	R	107 vertices $p = 0.003$	83	$b = -0.24$, $p < 0.001$	$b = 0.74$, $p < 0.001$	$b = -0.23$, $p = 0.005$	$b = -0.18$ (−0.34 −0.07) (*) $K^2 = 0.26$
MFG BA6 (35 −9 57)	R	53 vertices $p = 0.03$	53	$b = -0.39$, $p < 0.001$	$b = 0.57$, $p = 0.001$	$b = -0.18$, $p = 0.06$	$b = -0.23$ (−0.42 −0.08) (*) $K^2 = 0.28$

Rows illustrate simple mediation models to explain age-related effects on frontal SW density in the first NREMP with mean CT in each region as stand-alone mediators. The cluster column depicts the relationship between clusters and frontal SW density in the first NREM period when controlling for age. The conjunction analysis column depicts the path a effect and the number of vertices in each cluster linked to age effect. Coefficients in each path necessary for the computation of indirect effects are shown in designated columns. *b*-values refer to unstandardized parameter estimates of paths shown in Figure 1. Indirect effects are significant at $p < 0.05$ when 0 is not included in the 95% CI and significance is indicated with an asterisk. K^2 is an effect size of mediation and thus represents the proportion of the age-related effect on frontal SW density in the first NREMP that has been mediated by changes in CT (>0.25 = strong effect; >0.09 = medium effect; >0.001 = small effect). CT in each region is adjusted for ICV.

Table 12. Association between CT and frontal SW amplitude in the first NREMP and related mediation analyses

Total effect of age on frontal SW amplitude in the first NREMP (path c): $b = -0.08$, $p < 0.001$							
CT Cluster (BAs, peak)	Lat	Cluster size (corrected p-value)	Conjunct vertices (age and SW)	Parameter estimates (simple mediation models) Path a	Path b	Path c′	Indirect effects
SPL (27 −48 65) BA7	R	326 vertices $p < 0.001$	326	$b = -0.23$, $p < 0.001$	$b = 0.13$, $p < 0.001$	$b = -0.05$, $p = 0.001$	$b = -0.03$ (−0.05 −0.01) (*) $K^2 = 0.25$
Cuneus (−12 −88 33) BA19	L	410 vertices $p = 0.002$	59	$b = -0.17$, $p < 0.001$	$b = 0.13$, $p < 0.001$	$b = -0.08$, $p < 0.001$	$b = -0.02$ (−0.04 −0.01) (*) $K^2 = 0.19$
MFG (31 −11 60) BA6	R	67 vertices $p = 0.01$	67	$b = -0.37$, $p < 0.001$	$b = 0.12$, $p < 0.001$	$b = -0.03$, $p = 0.04$	$b = -0.04$ (−0.07 −0.02) (*) $K^2 = 0.32$
IPL (−57 −23 22) BA40/43	L	137 vertices $p = 0.05$	86	$b = -0.15$, $p < 0.001$	$b = 0.15$, $p = 0.002$	$b = -0.06$, $p < 0.001$	$b = -0.02$ (−0.05 −0.01) (*) $K^2 = 0.19$

Rows illustrate simple mediation models to explain age-related effects on frontal SW amplitude in the first NREMP with mean CT in each region as stand-alone mediators. The cluster column depicts the relationship between clusters and frontal SW amplitude in the first NREM period when controlling for age. The conjunction analysis column depicts the path a effect and the number of vertices in each cluster linked to age effect. Coefficients in each path necessary for the computation of indirect effects are shown in designated columns. *b-values* refer to unstandardized parameter estimates of paths shown in Figure 1. Indirect effects are significant at $p < 0.05$ when 0 is not included in the 95% CI and significance is denoted with an asterisk. K^2 is an effect size of mediation and thus represents the proportion of the age-related effect on frontal SW amplitude in the first NREMP that has been mediated by changes in CT (>0.25 = strong effect; >0.09 = medium effect; >0.001 = small effect). CT in each region is adjusted for ICV.

Table 13. Parallel mediation results (SW density in frontal derivations during first NREMP)

Effects	Significance of effects b, 95% CI, p value	Change in variance between models $\delta F_{(df)}$, δR^2, p value
Model 1 (initial model)		$\delta F_{(1,60)} = 28.93$, $\delta R^2 = 0.32$, $p < 0.001$
Total effect of age on SW density$_{(path\ c)}$	$b = -0.41$, (−0.56 −0.26), $p < 0.001$	
Model 2 (parallel mediation model)		$\delta F_{(2,58)} = 13.11$, $\delta R^2 = 0.21$, $p_{(\delta F)} < 0.001$
Direct effect of age on SW density$_{(path\ c')}$	$b = -0.10$, $p = 0.28$	
Total indirect effect of age on SW density mediated by changes in CT$_{(path\ a \times path\ b)}$	$b = -0.31$, (−0.50 −0.15) (*)	
Specific indirect effects of age on SW density (in model 2) mediated by		
Changes in MFG$_{(path\ a \times path\ b)}$	$b = -0.16$, (−0.33 −0.04) (*)	
Changes in IT$_{(path\ a \times path\ b)}$	$b = -0.15$, (−0.29 −0.04) (*)	

Total effects of age on frontal SW density during the first NREMP in the initial model (model 1; path c) compared with indirect and residual (direct) effects of age on SW density during the first NREMP in a parallel mediation model (model 2). $F\delta$ and $R\delta^2$ for model 1 refer to the variance explained by the age-only model compared with a constant, whereas values for model 2 refer to variance explained in model 2 (effects of age on frontal SW density in the first NREM period as mediated by specific changes in CT in different cortical regions) compared with the variance explained in model 1 (effect of age on frontal SW density in the first NREM period without considering CT). Individual coefficients in each path for each mediator are not shown; only significance for indirect effects are shown. Note that path a coefficients are the same as in Table 11, whereas path b coefficients are adjusted in the model when all mediators are included simultaneously. Indirect effects are significant at $p < 0.05$ when 0 is not included in the 95% CI and significance is denoted with an asterisk. CT is adjusted for ICV in these models.

plained variance in frontal SW density reached 54% when considering age and mediators altogether. We observed specific indirect effects in both the right MFG and IT. Moreover, contrast between these two indirect effects was not significant ($b = 0.03$, 95% CI: [−0.13 0.21]), indicating that age-related changes in frontal SW density during the first NREMP involve thinning in both cortical regions. Importantly, age did not present any residual direct effect on frontal SW density in this model.

Table 14 shows the parallel mediation analysis, which models how cortical thinning in the right MFG and SPL and in the left cuneus and IPL explained lower frontal SW amplitude during the first NREMP in older subjects. Simultaneously entering age and the above-mentioned regions (related to age and SW) into a model predicting frontal SW amplitude during the first NREMP increased explained variance by 19% compared with the initial model containing only the total effects of age (path c, model 2 vs model 1, Table 14). Total explained variance in frontal SW amplitude during the first NREMP reached 56% when considering age and mediators altogether. There was a significant specific indirect effect of age on frontal SW amplitude during the first NREMP through CT changes in the right MFG. Age did not present any residual direct effect on frontal SW amplitude in this model.

Discussion

This study provides insights into the mechanisms underlying changes in SWs across adulthood. We show that cortical thinning in regions considered to be involved in SW generation and propagation explains the decrease of SW density and amplitude in older adults.

Table 14. Parallel mediation results (SW amplitude in frontal derivations during first NREMP)

Effects	Significance of effects b, 95% CI, p-value	Change in variance between models $\delta F_{(df)}$, δR^2, p value
Model 1 (initial model)		$\delta F_{(1,60)} = 35.74, \delta R^2 = 0.37, p < 0.001$
Total effect of age on SW amplitude$_{(path\ c)}$	$b = -0.08, (-0.10\ -0.05), p < 0.001$	
Model 2 (Parallel mediation model)		$\delta F_{(4,56)} = 6.34, \delta R^2 = 0.19, p_{(\delta F)} = 0.001$
Direct effect of age on SW amplitude $_{(path\ c')}$	$b = -0.03, p = 0.09$	
Total indirect effect of age on SW amplitude mediated by changes in CT$_{(path\ a \times path\ b)}$	$b = -0.05, (-0.06 - 0.01)$ (*)	
Specific indirect effects of age on SW (in model 2) amplitude mediated by		
Changes in SPL$_{(path\ a \times path\ b)}$	$b = -0.01, (-0.03\ 0.01)$, NS	
Changes in cuneus$_{(path\ a \times path\ b)}$	$b = -0.01, (-0.03\ 0.01)$, NS	
Changes in MFG$_{(path\ a \times path\ b)}$	$b = -0.03, (-0.06\ -0.01)$ (*)	
Changes in IPL$_{(path\ a \times path\ b)}$	$b = -0.01, (-0.03\ 0.02)$, NS	

Total effects of age on frontal SW amplitude during the first NREMP in the initial model (model 1; path c) compared with indirect and residual (direct) effects of age on frontal SW amplitude in a parallel mediation model (model 2). δF and δR^2 for model 1 refer to the variance explained by the age-only model compared with a constant, whereas values for model 2 refer to the variance explained in model 2 (effects of age on frontal SW amplitude in the first NREM period, as mediated by specific changes in CT in different cortical regions) compared with variance explained in model 1 (effect of age on frontal SW amplitude in the first NREM period without considering CT). Individual coefficients in each path for each mediator are not shown; only significance for indirect effects are shown. Note that path a coefficients are the same as in Table 12, whereas path b coefficients are adjusted in the model when all mediators are included simultaneously. Indirect effects are significant at $p < 0.05$ when 0 is not included in the 95% CI and significance is denoted with an asterisk. CT is adjusted for ICV in these models.

SW characteristics are associated with CT

A study in 36 adolescents showed that, when correcting for age, SWA in central derivations was associated with CT in frontal, parietal, and temporal regions (Buchmann et al., 2011b). However, these associations were not replicated in 20 adults, leading the investigators to hypothesize that the association between CT and SWA could be epiphenomenal of microscopic changes in neutrophil during adolescence (Buchmann et al., 2011a). Because we found that the relationship between SW characteristics and CT did not change between age groups in with 63 subjects, differences in sample size could have affected statistical power in previous studies.

When controlling for age, SW density in prefrontal, frontal, central, and parietal derivations was associated with CT in the MFG, in the insula, and around the lateral fissure (STL, IPL). Although higher SW density in frontal derivations was specifically associated with higher CT in inferotemporal structures, higher parietal SW density was specifically associated with CT in the cingulate. Previous studies in adolescents showed an association between central SWA and CT in different frontal, temporal, cingulate, and parietal areas (Buchmann et al., 2011b). Interestingly, SWs frequently originate in the insula, STL, cingulate, or around the lateral fissure (including parts of the temporal, parietal, and frontal cortices) before involving other areas of the DMN (Murphy et al., 2009). Therefore, our results suggest that CT differences in regions facilitating SW production predict SW density.

When controlling for age, higher SW amplitude in both prefrontal and frontal derivations was associated with higher CT in the cuneus, whereas higher SW amplitude in both frontal and central derivations was associated with higher CT in the SPL. Higher frontal SW amplitude was also associated with higher CT in the MFG and lingual cortex, whereas higher parietal SW amplitude was associated with higher CT in the medial prefrontal cortex (mPFC). These regions are known to serve as the brain's "hubs" and facilitate long-range communication inside and outside of the DMN (van den Heuvel and Sporns, 2011; van den Heuvel et al., 2012). Once generated around the insula, surface SW amplitude increases as their source activity spreads along hubs in the DMN (Murphy et al., 2009). Moreover, small surface SW amplitude reflects local synchronized firing in regions underlying SWs, whereas large surface SW amplitude reflects global cortical synchrony (Nir et al., 2011). Furthermore, animal studies showed that the integrity of intracortical linkages allows for synchronization of activity during SWs (Amzica and Steriade, 1995; Wester and Contreras, 2012). Our results suggest that higher CT in those hubs facilitates cortical synchronization during SWs, leading to larger wave amplitude.

Surprisingly, SW amplitude in prefrontal and frontal derivations was associated with CT in posterior brain areas such as the SPL and cuneus. Previous studies also reported an association between posterior gray matter and frontal SW amplitude (Saletin et al., 2013). During their propagation, SWs act as waxing and waning waves, progressively increasing in amplitude and synchronizing more cortical regions (Massimini et al., 2004; Nir et al., 2011). Moreover, SWs can propagate following either an anteroposterior or a posteroanterior axis (Murphy et al., 2009). Importantly, whereas SWs originating from anterior sites stay preferentially in anterior regions, posteriorly generated SWs reach anterior regions easily (Menicucci et al., 2009). Therefore, large amplitude SWs in anterior regions reflect SWs that originate both from anterior and posterior regions. Presumably, higher posterior CT could facilitate cortical synchronization and SW amplitude buildup as they propagate from posterior to anterior regions, leading to maximal amplitude in frontal electrodes.

Overall, our results suggest that: (1) interindividual differences in the microstructure of areas considered to be involved in SW production facilitate generation and a high density of SWs and (2) the integrity of cortical areas through which SWs spread facilitates cortical synchronization and the amplitude buildup that occurs during each wave.

Regional cortical thinning explains age-related changes in SW characteristics

We observed more prominent effects of age on SW characteristics in frontal derivations, as reported previously (Carrier et al., 2011). Here, we found that cortical thinning was involved in age-related decreases in SW density and amplitude in all derivations except occipital, but not in the decrease of SW slope. Higher SW slope is associated with synchronous recruitment of cortical neurons as they alternate between states (Vyazovskiy et al., 2009). Therefore, the age-related decrease in SW slope is hypothesized to represent a less synchronous neuronal entry into active and silent states (Carrier et al., 2011). Steepness of SW slope is associated with white matter in the temporal lobe and in frontal regions of young adults (Piantoni et al., 2013). Crucially, white matter in frontotemporal regions is sensitive to age-related changes (Salat et al., 2009); therefore, white matter changes could presumably compromise synchronous recruitment of neurons and drive a decrease in SW slope in older subjects.

Age-related decreases of SW density in prefrontal, central, and parietal derivations were explained by thinning in the insula, in

regions neighboring the lateral fissure, or in the cingulate. However, the predominant frontal decrease of SW density was linked to thinning in the MFG and in the ITG for both all-night and first NREMP. Indeed, frontal regions show prominent age-related thinning, which could affect the strength of cortical dipoles generating SWs locally, triggering a local decrease in SW amplitude and thus in detection rate (Fjell et al., 2009). In addition, SWs are homeostatically regulated by previous wake-related experiences. SW generation increases proportionally with wake quality and intensity (Tononi and Cirelli, 2014). Conversely, the predominance of age-related changes in frontal SWs (particularly in conditions of high sleep pressure, e.g., during first NREMP) is thought to reflect age-related impairments in frontal lobe function (Lafortune et al., 2012). Interestingly, frontal regions interact with the ITG to support verbal functioning and executive performance (Fiebach et al., 2007). Indeed, CT in temporofrontal structures predicts executive and verbal functioning in young and older adults (Liu et al., 2013, 2013; Burzynska et al., 2012). Crucially, frontal SW density correlates with verbal fluency in older adults (Lafortune et al., 2014). Therefore, age-related changes in frontal SW could additionally be driven by decreased cognitive performance (which is associated with cortical changes). Cortical thinning in regions neighboring the lateral fissure could globally disrupt SW generation, whereas degradation of frontotemporal regions would compromise the quality of the waking experience, triggering an additional decrease in SWs. Future studies will need to investigate the relationship among age-related changes in CT, cognition, and SWs.

We show that thinning in the cuneus, SPL, and mPFC explained age-related decreases in all-night SW amplitude in prefrontal, central, and parietal electrodes, respectively, whereas the age-related decrease in frontal SW amplitude for all-night and the first NREMP involved the MFG. Previous research showed that atrophy of the mPFC was involved in the age-related decrease of SWA, affecting memory consolidation (Mander et al., 2013). Our study shows that cortical thinning in a set of regions involved in SW propagation, including the mPFC, explains the decrease of SW amplitude in aging (Murphy et al., 2009). We propose that cortical thinning could compromise propagation of neural activity during SWs, reducing the buildup of their amplitude. Future studies should investigate the effects of aging on CT in relation to SW propagation.

SWs are not passive phenomena because they also facilitate learning (Marshall et al., 2006; Steriade, 2006). Interestingly, increasing evidence suggests that learning experience can lead to fast changes in CT (Engvig et al., 2010, 2011; Bezzola et al., 2011). Therefore, another hypothesis suggests that SW-related impairments in memory consolidation in aging could themselves change CT. Instead, age-related mechanisms independent of CT could drive changes in SWs. For example, increased inhibition and decreased excitation have been observed in aged brains (Luebke et al., 2004; Wong et al., 2006), which may affect SWs (Haider et al., 2006). Such modifications could possibly impair SW regulation, diminish overnight memory consolidation, and contribute to age-related changes in CT. Studies investigating the long-term effects of experimental SW induction on CT would help in our understanding of this causal sequence.

Some limitations of our study need to be considered. There was some variance across derivations in regions identified in relation to SW, but variability in statistical power prevents strong claims about these differences. In addition, it remains unknown whether anatomical associations between SW and CT differ in stage 2 sleep or in other states of consciousness (e.g., anesthesia or coma).

Conclusions

This study further supports the relationship between cortical structure and sleep SWs. Our results suggest that changes in gray matter throughout adulthood constitute a mechanism by which age affects SW oscillations. These changes in SWs could predispose to cognitive decline and underlie sleep fragmentation. Future studies should detail the functional substrate of age-related changes in SW generation and propagation by investigating experimental induction and source analysis of SWs in older subjects.

Notes

Supplemental material for this article is available at http://www.ceams-carsm.ca/en/DubeSupplementals.pdf. Optional tables depicting new results concerning topographical associations between SW at different derivations and CT are provided. This material has not been peer reviewed.

References

Ad-Dab'bagh Y, Einarson D, Lyttelton O, Muehlboeck JS, Mok K, Ivanov O, Vincent RD, Lepage C, Lerch J, Fombonne E, Evans AC (2006) The CIVET image-processing environment: a fully automated comprehensive pipeline for anatomical neuroimaging research. In: Proceedings of the 12th Annual Meeting of the Organization for Human Brain Mapping, (Corbetta M, ed.). Florence, Italy, Neuroimage.

Aeschbach D, Borbély AA (1993) All-night dynamics of the human sleep EEG. J Sleep Res 2:70–81. CrossRef Medline

American Psychiatric Association (2000) Diagnostic and statistical manual of mental disorders. Washington, DC: APA.

Amzica F, Steriade M (1995) Disconnection of intracortical synaptic linkages disrupts synchronization of a slow oscillation. J Neurosci 15:4658–4677. Medline

Beck AT, Epstein N, Brown G, Steer RA (1988) An inventory for measuring clinical anxiety: psychometric properties. Journal of Consulting and Clinical Psychology 56:893–897. CrossRef Medline

Bezzola L, Mérillat S, Gaser C, Jäncke L (2011) Training-induced neural plasticity in golf novices. J Neurosci 31:12444–12448. CrossRef Medline

Brunner DP, Vasko RC, Detka CS, Monahan JP, Reynolds CF 3rd, Kupfer DJ (1996) Muscle artifacts in the sleep EEG: automated detection and effect on all-night EEG power spectra. J Sleep Res 5:155–164. CrossRef Medline

Buchmann A, Kurth S, Ringli M, Geiger A, Jenni OG, Huber R (2011a) Anatomical markers of sleep slow wave activity derived from structural magnetic resonance images. J Sleep Res 20:506–513. CrossRef Medline

Buchmann A, Ringli M, Kurth S, Schaerer M, Geiger A, Jenni OG, Huber R (2011b) EEG sleep slow-wave activity as a mirror of cortical maturation. Cereb Cortex 21:607–615. CrossRef Medline

Burzynska AZ, Nagel IE, Preuschhof C, Gluth S, Bäckman L, Li, SC, Lindenberger U, Heekeren HR (2012) Cortical thickness is linked to executive functioning in adulthood and aging. Hum Brain Mapp 33:1607–1620. CrossRef Medline

Carrier J, Viens I, Poirier G, Robillard R, Lafortune M, Vandewalle G, Martin N, Barakat M, Paquet J, Filipini D (2011) Sleep slow wave changes during the middle years of life. Eur J Neurosci 33:758–766. CrossRef Medline

Chauvette S, Volgushev M, Timofeev I (2010) Origin of active states in local neocortical networks during slow sleep oscillation. Cereb Cortex 20:2660–2674. CrossRef Medline

Collins DL, Peters TM, Evans AC (1994) Automated 3D nonlinear deformation procedure for determination of gross morphometric variability in human brain. Visualization in Biomedical Computing 2359:180–190.

Dang-Vu TT, Schabus M, Desseilles M, Albouy G, Boly M, Darsaud A, Gais S, Rauchs G, Sterpenich V, Vandewalle G, Carrier J, Moonen G, Balteau E, Degueldre C, Luxen A, Phillips C, Maquet P (2008) Spontaneous neural activity during human slow wave sleep. Proc Natl Acad Sci U S A 105:15160–15165. CrossRef Medline

Engvig A, Fjell AM, Westlye LT, Moberget T, Sundseth Ø, Larsen VA, Walhovd KB (2010) Effects of memory training on cortical thickness in the elderly. Neuroimage 52:1667–1676. CrossRef Medline

Fiebach CJ, Friederici AD, Smith EE, Swinney D (2007) Lateral inferotemporal cortex maintains conceptual-semantic representations in verbal working memory. J Cogn Neurosci 19:2035–2049. CrossRef Medline

Fjell AM, Westlye LT, Amlien I, Espeseth T, Reinvang I, Raz N, Agartz I, Salat DH, Greve DN, Fischl B, Dale AM, Walhovd KB (2009) High consistency of regional cortical thinning in aging across multiple samples. Cereb Cortex 19:2001–2012. CrossRef Medline

Grabner G, Janke AL, Budge MM, Smith D, Pruessner J, Collins DL (2006) Symmetric atlasing and model based segmentation: an application to the hippocampus in older adults. Medical image computing and computer-assisted intervention: MICCAI. International Conference on Medical Image Computing and Computer-Assisted Intervention 9:58–66.

Haider B, Duque A, Hasenstaub AR, McCormick DA (2006) Neocortical network activity in vivo is generated through a dynamic balance of excitation and inhibition. J Neurosci 26:4535–4545. CrossRef Medline

Hayes AF (2013) Introduction to mediation, moderation, and conditional process analysis. New York: Guilford.

Iber C, Ancoli-Israel S, Chesson A, Quan S (2007) The AASM manual for the scoring of sleep and associated events. Westchester, IL: American Academy of Sleep Medicine.

Kim JS, Singh V, Lee JK, Lerch J, Ad-Dab'bagh Y, MacDonald D, Lee JM, Kim SI, Evans AC (2005) Automated 3-D extraction and evaluation of the inner and outer cortical surfaces using a Laplacian map and partial volume effect classification. Neuroimage 27:210–221. CrossRef Medline

Lafortune M, Gagnon JF, Latreille V, Vandewalle G, Martin N, Filipini D, Doyon J, Carrier J (2012) Reduced slow-wave rebound during daytime recovery sleep in middle-aged subjects. PLoS One 7:e43224. CrossRef Medline

Lafortune M, Gagnon JF, Martin N, Latreille V, Dubé J, Bouchard M, Bastien C, Carrier J (2014) Sleep spindles and rapid eye movement sleep as predictors of next morning cognitive performance in healthy middle-aged and older participants. J Sleep Res 23:159–167. Medline

Landolt HP, Borbély AA (2001) Age-dependent changes in sleep EEG topography. Clin Neurophysiol 112:369–377. CrossRef Medline

Liu ME, Huang CC, Hwang JP, Yang AC, Tu PC, Yeh HL, Hong CJ, Liou YJ, Chen JF, Lin CP, Tsai SJ (2013) Effect of Bcl-2 rs956572 SNP on regional gray matter volumes and cognitive function in elderly males without dementia. AGE 35:343–352. Medline

Liu ME, Huang CC, Yang AC, Tu PC, Yeh HL, Hong CJ, Chen JF, Liou YJ, Lin CP, Tsai SJ (2013) Effect of Bcl-2 rs956572 Polymorphism on age-related gray matter volume changes. PLoS One 8:e56663. CrossRef Medline

Luebke JI, Chang YM, Moore TL, Rosene DL (2004) Normal aging results in decreased synaptic excitation and increased synaptic inhibition of layer 2/3 pyramidal cells in the monkey prefrontal cortex. Neuroscience 125:277–288. CrossRef Medline

MacDonald D, Kabani N, Avis D, Evans AC (2000) Automated 3-D extraction of inner and outer surfaces of cerebral cortex from MRI. Neuroimage 12:340–356. CrossRef Medline

Mander BA, Rao V, Lu B, Saletin JM, Lindquist JR, Ancoli-Israel S, Jagust W, Walker MP (2013) Prefrontal atrophy, disrupted NREM slow waves and impaired hippocampal-dependent memory in aging. Nat Neurosci 16:357–364. CrossRef Medline

Marshall L, Helgadóttir H, Mölle M, Born J (2006) Boosting slow oscillations during sleep potentiates memory. Nature 444:610–613. CrossRef Medline

Massimini M, Huber R, Ferrarelli F, Hill S, Tononi G (2004) The sleep slow oscillation as a traveling wave. J Neurosci 24:6862–6870. CrossRef Medline

Menicucci D, Piarulli A, Debarnot U, d'Ascanio P, Landi A, Gemignani A (2009) Functional structure of spontaneous sleep slow oscillation activity in humans. PLoS One 4:e7601. CrossRef Medline

Murphy M, Riedner BA, Huber R, Massimini M, Ferrarelli F, Tononi G (2009) Source modeling sleep slow waves. Proc Natl Acad Sci U S A 106:1608–1613. CrossRef Medline

Nir Y, Staba RJ, Andrillon T, Vyazovskiy VV, Cirelli C, Fried I, Tononi G (2011) Regional slow waves and spindles in human sleep. Neuron 70:153–169. CrossRef Medline

Paus T, Keshavan M, Giedd JN (2008) Why do many psychiatric disorders emerge during adolescence? Nat Rev Neurosci 9:947–957. Medline

Piantoni G, Poil SS, Linkenkaer-Hansen K, Verweij IM, Ramautar JR, Van Someren EJ, Van Der Werf YD (2013) Individual differences in white matter diffusion affect sleep oscillations. J Neurosci 33:227–233. CrossRef Medline

Preacher KJ, Kelley K (2011) Effect size measures for mediation models: quantitative strategies for communicating indirect effects. Psychological Methods 16:93–115. CrossRef Medline

Salat DH, Buckner RL, Snyder AZ, Greve DN, Desikan RS, Busa E, Morris JC, Dale AM, Fischl B (2004) Thinning of the cerebral cortex in aging. Cereb Cortex 14:721–730. CrossRef Medline

Salat DH, Greve DN, Pacheco JL, Quinn BT, Helmer KG, Buckner RL, Fischl B (2009) Regional white matter volume differences in nondemented aging and Alzheimer's disease. Neuroimage 44:1247–1258. CrossRef Medline

Saletin JM, van der Helm E, Walker MP (2013) Structural brain correlates of human sleep oscillations. Neuroimage 83:658–668. CrossRef Medline

Schüz A, Palm G (1989) Density of neurons and synapses in the cerebral cortex of the mouse. J Comp Neurol 286:442–455. CrossRef Medline

Sled JG, Zijdenbos AP, Evans AC (1998) A nonparametric method for automatic correction of intensity nonuniformity in MRI data. IEEE Trans Med Imaging 17:87–97. CrossRef Medline

Steriade M (2006) Grouping of brain rhythms in corticothalamic systems. Neuroscience 137:1087–1106. CrossRef Medline

Steriade M, Contreras D, Curró Dossi R, Nuñez A (1993a) The slow (< 1 Hz) oscillation in reticular thalamic and thalamocortical neurons: scenario of sleep rhythm generation in interacting thalamic and neocortical networks. J Neurosci 13:3284–3299. Medline

Steriade M, Nuñez A, Amzica F (1993b) A novel slow (< 1 Hz) oscillation of neocortical neurons in vivo: depolarizing and hyperpolarizing components. J Neurosci 13:3252–3265. Medline

Tohka J, Zijdenbos A, Evans A (2004) Fast and robust parameter estimation for statistical partial volume models in brain MRI. Neuroimage 23:84–97. CrossRef Medline

Tononi G, Cirelli C (2014) Sleep and the price of plasticity: from synaptic and cellular homeostasis to memory consolidation and integration. Neuron 81:12–34. CrossRef Medline

van den Heuvel MP, Sporns O (2011) Rich-club organization of the human connectome. J Neurosci 31:15775–15786. CrossRef Medline

van den Heuvel MP, Kahn RS, Goñi J, Sporns O (2012) High-cost, high-capacity backbone for global brain communication. Proc Natl Acad Sci U S A 109:11372–11377. CrossRef Medline

Volgushev M, Chauvette S, Mukovski M, Timofeev I (2006) Precise long-range synchronization of activity and silence in neocortical neurons during slow-wave oscillations [corrected]. J Neurosci 26:5665–5672. CrossRef Medline

Vyazovskiy VV, Harris KD (2013) Sleep and the single neuron: the role of global slow oscillations in individual cell rest. Nat Rev Neurosci 14:443–451. Medline

Vyazovskiy VV, Olcese U, Lazimy YM, Faraguna U, Esser SK, Williams JC, Cirelli C, Tononi G (2009) Cortical firing and sleep homeostasis. Neuron 63:865–878. CrossRef Medline

Wester JC, Contreras D (2012) Columnar interactions determine horizontal propagation of recurrent network activity in neocortex. J Neurosci 32:5454–5471. CrossRef Medline

Wong TP, Marchese G, Casu MA, Ribeiro-da-Silva A, Cuello AC, De Koninck Y (2006) Imbalance towards inhibition as a substrate of aging-associated cognitive impairment. Neurosci Lett 397:64–68. CrossRef Medline

Worsley KJ, Taylor JE, Tomaiuolo F, Lerch J (2004) Unified univariate and multivariate random field theory. Neuroimage 23:S189–S195. CrossRef Medline

Zhao L, Boucher M, Rosa-Neto P, Evans AC (2013) Impact of scale space search on age- and gender-related changes in MRI-based cortical morphometry. Hum Brain Mapp 34:2113–2128. CrossRef Medline